ANTIMICROBIAL AGENTS AND CHEMOTHERAPY, Oct. 2007, p. 3562–3567 Vol. 51, No. 10
0066-4804/07/$08.00+0 doi:10.1128/AAC.00383-07

Targeting Fatty Acid Biosynthesis for the Development of Novel Chemotherapeutics against *Mycobacterium tuberculosis*: Evaluation of A-Ring-Modified Diphenyl Ethers as High-Affinity InhA Inhibitors▽†

Melissa E. Boyne,[1] Todd J. Sullivan,[2] Christopher W. amEnde,[2] Hao Lu,[2] Veronica Gruppo,[1] Darragh Heaslip,[1] Anita G. Amin,[1] Delphi Chatterjee,[1] Anne Lenaerts,[1] Peter J. Tonge,[2]* and Richard A. Slayden[1,3]*

Rocky Mountain Regional Center of Excellence[3] and Department of Microbiology, Immunology and Pathology,[1] Colorado State University, Fort Collins, Colorado 80523-1682, and Department of Chemistry, Stony Brook University, Stony Brook, New York 11794-3400[2]

Received 21 March 2007/Returned for modification 14 April 2007/Accepted 20 July 2007

Structure-based design was used to develop a focused library of A-ring-modified diphenyl ether InhA inhibitors. From this library of analogs, two high-affinity alkyl-substituted diphenyl ethers, 6PP and 8PP, were selected for advanced study into their in vitro activity against *Mycobacterium tuberculosis* clinical isolates, their in vivo properties, and their signature response mode of action. 6PP and 8PP demonstrated enhanced activity against whole bacteria and showed activity in a rapid macrophage model of infection. In addition, transcriptional profiling revealed that the A-ring modifications of 6PP and 8PP increased the specificity of each analog for InhA. Both analogs had substantially longer half-lives in serum than did the parent compound, exhibited a fivefold reduction in cytotoxicity compared to the parent compound, and were well tolerated when administered orally at 300 mg/kg of body weight in animal models. Thus, the A-ring modifications increased the affinity and whole-cell specificity of the compounds for InhA and increased their bioavailability. The next step in optimization of the pharmacophore for preclinical evaluation is modification of the B ring to increase the bioavailability to that required for oral delivery.

Isoniazid (INH) is the single most effective chemotherapeutic for the treatment of tuberculosis. While the exquisite potency of INH may result from a complex mode of action that still remains to be delineated completely (15), it is known that INH affects cell wall biosynthesis via alterations of the mycobacterial type II fatty acid biosynthesis (FAS-II) pathway, one mechanism of which is through inhibition of InhA, the FAS-II enoyl reductase (1, 13, 15, 19). Although INH resistance is associated with mutations in InhA as well as KasA and the upstream regulatory region of the *mabA-inhA* operon (12, 15, 19), the vast majority of INH-resistant isolates contain mutations in the KatG catalase peroxidase protein responsible for the activation of INH (2, 9, 14, 15). Consequently, novel compounds with a distinct pharmacophore that inhibits InhA but does not require activation by KatG hold promise for the treatment of multidrug-resistant (MDR) clinical strains of *Mycobacterium tuberculosis*.

Previously, we reported the synthesis of compounds designed to explore the diphenyl ether pharmacophore as a potential antitubercular agent. These studies were based on the known ability of triclosan to inhibit the enoyl reductase class of enzymes (20). Using rational drug development strategies, this initial study substantiated the use of modeling, enzyme inhibition, and whole-cell assays to identify compounds with enhanced activity against clinical strains of *M. tuberculosis* with various drug resistance profiles. However, it did not address the whole bacterial mode of action, toxicity, or in vivo activity of the compounds. Accordingly, the work presented here expands on our previous report by investigation of the mode of action and potential detoxification transcriptional patterns of the most potent analogs identified and by analysis of their efficacy in models of infection. Our findings demonstrate that although these high-affinity InhA inhibitors have issues with low bioavailability, they are more effective in vitro inhibitors with less cytotoxicity than the parent compound triclosan, thus narrowing the spectrum of structural changes required for drug enhancement. The transcriptional responses confirm that the alkyl diphenyl ethers inhibit InhA within the cell, unlike triclosan, which likely has other targets (6). The identification of a transcriptional response specific to the inhibition of InhA will be critical for the development of the next generation of high-affinity InhA inhibitors with improved in vivo properties.

* Corresponding author. Mailing address for Richard A. Slayden: Department of Microbiology, Immunology and Pathology, Colorado State University, Fort Collins, CO 80523-1682. Phone: (970) 491-2902. Fax: (970) 491-1815. E-mail: richard.slayden@colostate.edu. Mailing address for Peter J. Tonge: Department of Chemistry, Stony Brook University, Stony Brook, NY 11794-3400. Phone: (631) 632-7907. Fax: (631) 632-7934. E-mail: peter.tonge@sunysb.edu.

† Supplemental material for this article may be found at http://aac.asm.org/.

▽ Published ahead of print on 30 July 2007.

MATERIALS AND METHODS

MIC determinations and cytotoxicity testing. MICs were determined using the microplate dilution method as previously described (16). African green monkey kidney cells (Vero cells) were grown in RPMI 1640 medium supplemented with 1.5 g/liter sodium bicarbonate, 10 ml/liter 100 mM sodium pyruvate, 140 ml/liter

100× nonessential amino acids, 100 ml/liter penicillin-streptomycin solution (10,000 IU/10,000 μg/ml), and 10% bovine calf serum at 37°C in a 5% CO_2 incubator with 75% humidity. Testing was conducted for 72 h at 37°C in a 5% CO_2 incubator. Cells were washed, CellTiter 96 AQueous One solution was added to each well, and plates were incubated for 4 h at 37°C. Plates were read at 490 nm using a spectrophotometric plate reader, and the absorbance readings were used to calculate the 50% lethal concentration (LC_{50}).

Rapid macrophage assay. A rapid macrophage assay was developed to assess the activities of compounds against intracellular bacteria. J774A.1 cells were allowed to phagocytose *M. tuberculosis* H37Rv cells (multiplicity of infection of 1:10) for 4 h at 37°C and then washed four times with phosphate-buffered saline (PBS) and culture growth medium without (control) or with one of the two most potent compounds (6PP and 8PP) at the MIC or twice the MIC (2× MIC). At time zero and 1 and 4 days postinfection, triplicate monolayers per compound were washed four times with PBS, lysed by the addition of 0.1% Triton X-100, and plated on 7H11 medium. Following incubation at 37°C, CFU were enumerated.

In vivo evaluation. The oral bioavailability of the compounds was tested using a bioassay approach, as described before (8). Eight to 10-week-old female C57BL/6 mice were dosed via oral gavage. Twenty minutes, 1 h, 2 h, and 4 h after being dosed, three mice were bled from the tail vein. Sera and standards of the compounds were tested in threefold dilutions against *M. tuberculosis* H37Rv. Bacterial growth was determined by measuring the optical density after 3, 6, 9, and 12 days. Estimations of serum drug levels (in $\mu g\ ml^{-1}$ serum) were obtained by using the MIC data from the standard drug lanes.

Transcriptional profiling. *M. tuberculosis* H37Rv was treated with 15 μM 6PP, 12 μM 8PP, or 86 μM triclosan or left untreated at 37°C with shaking for 2 h. Whole bacteria were subjected to TRIzol extraction, and total RNA was isolated by physical disruption. Microarray analysis was performed with labeled cDNAs generated using direct labeling from 5 μg of total RNA as described previously (17). The resulting fluorescence for each channel of the array (Cy3 and Cy5) was normalized to the mean channel intensity and analyzed using Genesifter analysis software. *t* test statistical analysis and Benjamini and Hochberg correction were applied to all analyses of all mean normalized data. Significance was considered to be a >1.5-fold alteration in expression, with a *P* value cutoff of <0.05. The transcriptional activity of selected genes identified by DNA microarray analysis was verified using real-time PCR as described previously (20).

RESULTS

Determination of 6PP and 8PP activities against clinical MDR strains. We previously reported whole bacterial activity of a series of alkyl-disubstituted diphenyl ethers against the laboratory strain H37Rv and five clinical *M. tuberculosis* strains (Table 1) (20). The two most potent compounds, 6PP and 8PP, were nanomolar inhibitors of InhA and had MICs of 1 to 2 μg/ml against drug-sensitive and drug-resistant *M. tuberculosis.* In general, gene dosage increased the MICs for all compounds; however, the MIC was influenced more for analogs substituted with short-chain alkyl groups than for triclosan or any of the long-chain-substituted compounds (Table 1). This observation indicates that there is a narrow range of alkyl substitutions that provide greater whole-cell specificity for InhA.

Evaluation of cytotoxicity of diphenyl ether analogs. The diphenyl ether analogs with MICs of <50 μg/ml were tested for general cytotoxicity using a Vero cell line (Table 1). Many of the compounds had LC_{50} values at their MIC concentration. However, 6PP and 8PP had LC_{50} values of 13 μg/ml and 10 μg/ml, resulting in therapeutic indexes of 6 and 5, respectively. In contrast, the parent compound had an LC_{50} at or below the MIC, resulting in a measurable therapeutic index of 1.

Assessment of serum binding and of activity in a rapid macrophage assay. To evaluate whether protein binding alters the activities of 6PP and 8PP and whether they are able to inhibit the growth of intracellular *M. tuberculosis*, the MICs of these compounds were determined in the presence of 10%

TABLE 1. MICs and toxicity of alkyl diphenyl ethers[a]

Compound	MIC_{99}, $\mu g\ ml^{-1}$ (μM)							LC_{50} ($\mu g\ ml^{-1}$)	Therapeutic index
	H37Rv	pMH29:InhA	W210	TN587	NHN20	HN335-2	NHN382		
Triclosan	12.5 ± 0 (43.1 ± 0)	33.3 ± 12.9 (115 ± 45)	14.7 ± 3.8 (50.8 ± 13)	12.5 ± 0 (43.1 ± 0)	12.5 ± 0 (43.1 ± 0)	18.8 ± 6.3 (64.9 ± 21.7)	12.5 ± 0 (43.1 ± 0)	<12.5	<1
2PP	15.6 ± 7.7 (72.9 ± 35.7)	133.3 ± 57.7 (622.3 ± 269.5)	10.4 ± 3.2 (48.6 ± 15.1)	8.9 ± 4.2 (41.3 ± 19.4)	14.6 ± 8.5 (68.1 ± 39.9)	6.3 ± 53.4 (629.2 ± 16)	10.4 ± 3.2 (48.6 ± 15.1)	<15.6	<1
4PP	2.6 ± 0.8 (10.8 ± 3.3)	50.0 ± 0 (206.4 ± 0)	2.6 ± 0.8 (10.8 ± 3.3)	2.1 ± 0.8 (8.7 ± 3.3)	2.1 ± 0.9 (8.7 ± 3.3)	2.8 ± 0.7 (11.6 ± 2.8)	3.8 ± 1.4 (15.5 ± 5.8)	1.6	<1
5PP	4.2 ± 1.6 (116.3 ± 6.3)	50.0 ± 0 (195.1 ± 0)	1.6 ± 0 (6.2 ± 0)	1.6 ± 1 (6.2 ± 0)	1.6 ± 2 (6.2 ± 0)	2.1 ± 0.8 (8.2 ± 3.1)	4.2 ± 1.6 (16.3 ± 6.3)	3.8	1
6PP	2.1 ± 0.9 (7.8 ± 3.3)	18.8 ± 6.8 (69 ± 25)	2.9 ± 0.4 (10.7 ± 1.5)	2.0 ± 1.0 (7.4 ± 3.7)	3.1 ± 0 (11.5 ± 0)	3.7 ± 0.9 (13.7 ± 3.3)	3.1 ± 0 (11.5 ± 0)	12.5	6
8PP	1.9 ± 0.5 (6.4 ± 1.7)	22.9 ± 5.1 (77 ± 17)	2.6 ± 0.4 (8.7 ± 1.3)	2.0 ± 1.0 (6.7 ± 3.4)	2.4 ± 0.76 (8.0 ± 2.6)	3.1 ± 0 (10.4 ± 0)	2.6 ± 0.9 (8.7 ± 3.0)	9.9	5
9PP	14.1 ± 9.2 (45 ± 29.5)	50.0 ± 0 (160.0 ± 0)	8.3 ± 3.2 (26.7 ± 10.3)	7.3 ± 4.3 (23.3 ± 13.7)	16.7 ± 6.5 (53.3 ± 20.7)	12.5 ± 0 (40 ± 0)	4.7 ± 1.8 (15 ± 5.8)	<14.1	<1

[a] The laboratory strain *M. tuberculosis* H37Rv and clinical strains W210 (KatG wild type), TN587 (KatG-S315T), and NHN382 (KatG-Del), with differing drug resistance profiles, were used for MIC determinations. Toxicity was evaluated using Vero cells, and the therapeutic index was calculated as LC_{50}/MIC_{99}. Data are means ± standard deviations.

TABLE 2. Protein binding and bioavailability analysis of 6PP and 8PP[a]

Compound	Dose (mg kg^{-1})	Formulation	Method of compound delivery	MIC (μg ml^{-1})		Drug serum level (μg ml^{-1})	Serum absorption index
				Without serum	With serum		
6PP	300	Methylcellulose	Oral	3.3	3.3	66	20
6PP	300	Cyclodextrin	Oral	3.3	3.3	132	40
6PP	300	PBS	Subcutaneous	3.3	3.3	99	30
8PP	300	Methylcellulose	Oral	1.1	1.1	20	18
Triclosan	300	PBS	Subcutaneous	3.3	10	66	30
INH	25	H_2O	Oral	0.05	0.05	>13	>320

[a] In vitro MICs for H37Rv were determined within the bioavailability assay by broth microdilution. Serum (10%) was added to one set of controls to determine the effect of protein binding on the MIC. Drug levels in mouse serum were estimated by multiplying the dilution factor by the MIC of the drug in the absence of serum. The serum absorption index was calculated as the serum concentration divided by the MIC_{99} and is a measure of the bioavailability of the compound.

mouse serum (according to CLSI guidelines), and their activity against bacteria was evaluated in a rapid macrophage assay. The results showed that the MIC for 6PP or 8PP was not influenced by the presence of serum, indicating that neither of these compounds has serum binding problems (Table 2). Furthermore, the addition of 6PP or 8PP at the 2× MIC to macrophages containing *M. tuberculosis* resulted in bacterial growth inhibition of 73% ± 7% and 71% ± 1%, respectively, which is demonstrative of intracellular antimycobacterial activity. INH was included as a positive control and reduced growth by 98% ± 1% at the 2× MIC. The inhibitory activities of 6PP and 8PP against intracellular bacteria in the rapid macrophage model are similar to those observed for other compounds tested for activity against *M. tuberculosis* (18). It should also be noted that both 6PP and 8PP displayed much lower toxicity in the macrophage assay than did the parent compound, triclosan, which was lethal to macrophages after 1 day of treatment at both the MIC and 2× MIC levels.

Bioavailability and in vivo efficacy of 6PP and 8PP. As a prelude to more detailed in vivo studies, a bioavailability assay was performed to assess the serum levels of 6PP and 8PP after oral administration (8). Drug serum levels of 6PP and 8PP ranged from 66 to 132 μg/ml depending on the formulation (Table 2), resulting in serum absorption indices of 18 to 40. This is in contrast to INH, which had serum levels of >13 μg/ml, resulting in serum absorption indices of >320. Importantly, the presence of analogs could be detected in the serum 8 h after dosing, which is much longer than the time to detection reported for INH (3).

Transcriptional differences between triclosan, 6PP, and 8PP. Previous reports indicate that triclosan affects respiration in addition to fatty acid synthesis, which likely results because triclosan is only a modest InhA inhibitor and thus must be used at concentrations that elicit other cellular effects (6). In order to determine if the increased potencies of 6PP and 8PP towards InhA had narrowed the mode of action of these compounds, the global transcriptional response of H37Rv treated with 6PP, 8PP, or triclosan was assessed. These studies showed that triclosan had a more pleiotropic effect on bacterial metabolism than did treatment with either 6PP or 8PP (Table 3; see Tables S1 and S2 in the supplemental material). In particular, 6PP and 8PP upregulated hallmark genes associated with cell wall synthesis, including *fas*, the KAS operon, *accD4*, *pks13*, *pks16*, *fadD32*, and *rv0241c* (6), demonstrating that these compounds specifically target fatty acid biosynthesis. In contrast, triclosan failed to induce cell wall synthesis genes; rather, this compound induced a large number of genes involved in β-oxidation, including putative acyl-coenzyme A (acyl-CoA) synthase genes, genes for acyl-CoA dehydrogenases that catalyze the initiation of β-oxidation, and genes that encode β-oxidation proteins responsible for cyclic degradation of fatty acids. In addition, 6PP and 8PP also induced genes involved in meromycolate modification (*umaA*, *mmaA3*, and *mmaA4*), genes involved in the synthesis of arabinogalactan (*embA* and *embB*), the final cell wall acceptor for mycolic acids, and the gene for a member of the antigen 85 complex (*fpbC*) involved in deposition of mycolic acids (5).

Previously, we reported that 6PP and 8PP failed to upregulate a putative efflux pump (*rv1685c-rv1687c*) and aromatic dioxygenase (*rv3160c-rv3161c*) that were induced by triclosan. The additional studies reported here now show that, instead, 6PP and 8PP induce the expression of *iniABC*, an operon reported to encode at least one component of an undefined efflux mechanism that is known to be induced by and associated with tolerance to the cell wall inhibitors INH and ethambutol (7). Thus, the diphenyl ether analogs circumvent detoxification mechanisms associated with triclosan but may induce a potential efflux pump associated with drug tolerance. Fur-

TABLE 3. Summary of differentially regulated ORFs, according to functional classification, after drug treatment[a]

Drug	Total no. of ORFs analyzed	Total no. of differentially regulated ORFs[b]	No. (%) of differentially regulated ORFs									
			Cell wall and cell processes	Conserved hypothetical	Information pathways	Insertion sequences and phages	Intermediary metabolism and respiration	Lipid metabolism	PE/PPE	Regulatory proteins	Unknown	Virulence, detoxification, adaptation
Triclosan	2,498	722	93 (17)	145 (19)	77 (10)	15 (2)	15 (25)	62 (8)	33 (4)	25 (3)	107 (14)	20 (3)
6PP	737	127	21 (10)	31 (24)	4 (3)	3 (2)	27 (21)	11 (9)	3 (2)	12 (9)	7 (6)	8 (6)
8PP	780	121	12 (10)	38 (31)	2 (2)	4 (3)	15 (12)	14 (12)	4 (3)	13 (11)	14 (12)	5 (4)

[a] Functional classifications were those annotated by http://genolist.pasteur.fr/TubercuList/.
[b] ORFs with expression differences of ≥1.5-fold ($P > 0.05$).

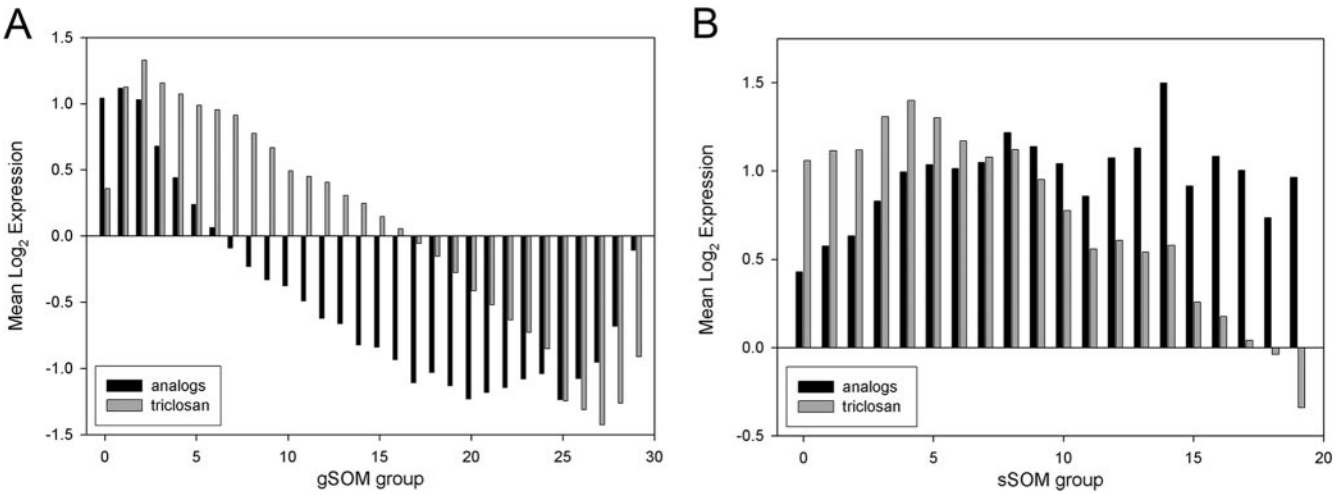

FIG. 1. Tandem-SOM analysis. (A) gSOM analysis of transcriptionally active ORFs. (B) sSOM analysis of ORFs from groups 0 to 2 of gSOM analysis. gSOM analysis distributed 3,627 ORFs into 30 groups (groups 0 to 29). sSOM analysis distributed 803 ORFs into 20 groups (groups 0 to 19).

thermore, treatment with 6PP and 8PP consistently caused increased transcription of *rv2846c* (*efpA*), encoding an efflux protein which leads to decreased susceptibility to INH when deleted in *Mycobacterium smegmatis* (11). This particular efflux protein was not upregulated in *M. tuberculosis* following treatment with the parent compound, triclosan. These studies again raise important differences between triclosan and the alkyl diphenyl ethers and also underline the similarity in transcriptional responses between the latter and cell wall biosynthesis inhibitors such as INH.

High-content multiple-feature profiles of high-affinity InhA inhibitors. Tandem self-organizing map (tandem-SOM) analysis was performed to identify open reading frames (ORFs) that can be used to construct high-content multiple-feature screens to monitor gene responses of next-generation diphenyl ethers (Fig. 1). When the signature response of *M. tuberculosis* to 6PP and 8PP treatment was studied and deciphered, genes ($n = 60$) that were uniquely responsive to treatment with diphenyl ethers ($\geq$1.5-fold change in expression) were grouped in global SOM (gSOM) groups 0 to 1 and genes that were induced by treatment with the analogs were grouped in sub-SOM (sSOM) groups 7 to 19. These genes are listed in Table 4 and include genes encoding fatty acid and mycolic acid synthases. This provides a signature profile for identifying novel compounds that have a similar mode of action to 6PP and 8PP.

DISCUSSION

The development of novel drugs against *M. tuberculosis* has numerous hurdles; among them are identification of therapeutically relevant metabolic targets, optimization of potency, reduction of toxicity, and introduction of favorable physiochemical characteristics. Although the mode of action of INH is arguably complex, it is clear that InhA is a validated target for drug discovery (1, 4, 10, 12, 15, 19). Therefore, our strategy is to utilize this knowledge to develop new InhA inhibitors that are distinct in structure from INH and thus do not require activation by KatG. Through molecular modeling and target-based screening, a series of diphenyl ethers were synthesized, leading to the identification of two compounds as potential antimycobacterial drug candidates (20).

An area of concern regarding the development of novel inhibitors against an established target is that these compounds might also be ineffective against existing drug-resistant strains. However, by synthesizing high-affinity InhA inhibitors that did not require KatG activation, both 6PP and 8PP were fully active against representative MDR clinical isolates with various resistance profiles. In addition, given the necessary long duration of treatment, toxicity is a significant issue with all antimycobacterial drugs. However, the A-ring modifications led to a >5-fold reduction in cytotoxicity compared to that of triclosan.

Lower toxicity levels were also apparent upon treatment of macrophages, as triclosan was toxic to macrophages, while 6PP and 8PP were not. Importantly, however, both 6PP and 8PP showed the ability to reduce bacterial growth in the rapid macrophage assay, thus indicating that these compounds were able to enter the macrophage and remain effective against intracellular *M. tuberculosis* growing under altered metabolic conditions. Given orally, neither 6PP nor 8PP had bioavailability as high as that of INH, but the analogs could be detected at 8 h postadministration. In addition, there were no adverse reactions noted upon oral administration, substantiating the reduced toxicity of these compounds. Importantly, the increased serum half-lives of 6PP and 8PP compared to that of INH are expected to provide more constant drug pressure, allowing greater dosing intervals during treatment. However, because of the poor bioavailability of 6PP and 8PP, neither demonstrated significant efficacy in a rapid mouse model when delivered by gavage (data not shown). Thus, while not active orally, these compounds exhibit decreased cytotoxicity and increased half-lives, which are crucial characteristics for any newly developed drug. Together, the in vivo studies indicate that 6PP and 8PP have low cytotoxicity levels and can inhibit intracellular organisms but still have limited bioavailability.

The next step in optimizing the drug activity of diphenyl

TABLE 4. High-content multiple-feature profiles of high-affinity InhA inhibitors[a]

ORF	Gene name	gSOM group	sSOM group	Ratio	*P* value	Protein name or function
Rv0129c	*fbpC2*	0	14	3.4	0.0049	Secreted antigen 85 complex C (FbpC)
Rv0171	Rv0171	0	15	1.5	0.0476	Mce family protein Mce1C
Rv0172	Rv0172	0	13	1.5	0.0217	Mce family protein Mce1D
Rv0179c	*lprO*	0	17	1.8	0.0070	Possible lipoprotein LprO
Rv0180c	Rv0180c	0	9	1.7	0.0107	Probable conserved transmembrane protein
Rv0181c	Rv0181c	1	8	1.7	0.0072	Hypothetical protein
Rv0197	Rv0197	0	13	1.7	0.0029	Possible oxidoreductase
Rv0342	*iniA*	0	15	1.5	0.0050	INH-inducible gene protein IniA
Rv0410c	*pknG*	0	17	1.5	0.0499	Serine/threonine protein kinase G (STPK G)
Rv0411c	*glnH*	0	16	1.8	0.0040	Probable glutamine-binding lipoprotein GlnH (GlnBP)
Rv0412c	Rv0412c	0	16	1.6	0.0044	Possible conserved membrane protein
Rv0474	Rv0474	0	13	2.4	0.0001	Probable transcriptional regulatory protein
Rv0676c	*mmpL5*	0	9	2.4	0.0043	Probable conserved transmembrane transport protein MmpL5
Rv0678	Rv0678	1	7	2.9	0.0163	Hypothetical protein
Rv0680c	Rv0680c	0	8	1.7	0.0225	Probable conserved transmembrane protein
Rv0724	*sppA*	0	12	1.6	0.0007	Possible protease IV SppA (endopeptidase IV)
Rv0805	Rv0805	0	13	1.5	0.0050	Hypothetical protein
Rv0846c	Rv0846c	0	14	1.7	0.0046	Probable oxidase
Rv0896	*gltA2*	0	10	1.5	0.0246	Citrate synthase
Rv0932c	*pstS*	0	14	1.6	0.0172	Periplasmic phosphate-binding lipoprotein PstS2 (PBP-2)
Rv1022	*lpqU*	1	7	2.3	0.0256	Probable conserved lipoprotein LpqU
Rv1130	Rv1130	0	17	3.9	0.0117	Hypothetical protein
Rv1131	Rv1131	0	19	2.5	0.0001	Citrate synthase
Rv1157c	Rv1157c	0	16	2.0	0.0037	Conserved hypothetical Ala-, Pro-rich protein
Rv1158c	Rv1158c	0	16	2.2	0.0116	Conserved hypothetical Ala-, Pro-rich protein
Rv1218c	Rv1218c	0	12	1.6	0.0001	ATP-binding protein ABC transporter
Rv1286	*cysN*	0	9	2.5	0.0341	Bifunctional sulfate adenylyltransferase
Rv1292	*argS*	0	10	1.5	0.0326	Arginyl-tRNA synthetase
Rv1397c	Rv1397c	0	16	1.5	0.0045	Hypothetical protein
Rv1416	*ribH*	1	7	1.8	0.0251	Riboflavin synthase subunit beta
Rv1497	*lipL*	0	13	1.7	0.0009	Probable esterase LipL
Rv1548c	*PPE*	0	12	1.5	0.0413	PPE family protein
Rv1690	*lprJ*	0	11	2.1	0.0008	Probable lipoprotein LprJ
Rv1702c	Rv1702c	1	7	1.7	0.0266	Hypothetical protein
Rv1782	Rv1782	0	13	1.5	0.0010	Probable conserved membrane protein
Rv1784	Rv1784	0	12	1.6	0.0007	Hypothetical protein
Rv1875	Rv1875	0	11	1.5	0.0167	Hypothetical protein
Rv1880c	Rv1880c	1	7	1.6	0.0344	Probable cytochrome P450 140 (CYP140)
Rv1912c	*fadB5*	1	8	3.0	0.0319	Possible oxidoreductase FadB5
Rv1945	Rv1945	0	10	1.8	0.0087	Hypothetical protein
Rv2053c	Rv2053c	0	10	2.1	0.0030	Probable transmembrane protein
Rv2193	*ctaE*	0	10	1.5	0.0445	Probable cytochrome *c* oxidase (subunit III) (CtaE)
Rv2234	*ptpA*	1	8	1.5	0.0144	Phosphotyrosine protein phosphatase PtpA
Rv2454c	Rv2454c	0	12	1.5	0.0213	Ferrodoxin oxidoreductase beta subunit
Rv2516c	Rv2516c	0	8	2.2	0.0388	Hypothetical protein
Rv2963	Rv2963	0	15	1.7	0.0025	Probable integral membrane protein
Rv3140	*fadE23*	0	12	2.1	0.0005	Probable acyl-CoA dehydrogenase FadE23
Rv3159c	*PPE*	1	8	2.0	0.0367	PPE family protein
Rv3209	Rv3209	0	14	1.8	0.0016	Conserved hypothetical threonine- and proline-rich protein
Rv3249c	Rv3249c	0	14	2.0	0.0055	Transcriptional regulatory protein (probably TetR family)
Rv3251c	*rubA*	0	14	2.0	0.0020	Probable rubredoxin RubA
Rv3252c	Rv3252c	0	13	2.1	0.0008	Probable transmembrane alkane 1-monooxygenase AlkB
Rv3408	Rv3408	0	13	1.8	0.0161	Hypothetical protein
Rv3496c	Rv3496c	0	13	1.5	0.0121	Mce family protein Mce4D
Rv3500c	Rv3500c	0	8	2.1	0.0427	Conserved hypothetical integral membrane protein YrbE4B
Rv3740c	Rv3740c	0	19	1.6	0.0013	Hypothetical protein
Rv3741c	Rv3741c	0	19	2.9	0.0002	Possible oxidoreductase
Rv3810	*pirG*	0	12	2.2	0.0086	Exported repetitive protein precursor PirG (EXP53)
Rv3837c	Rv3837c	0	19	1.7	0.0117	Probable phosphoglycerate mutase

[a] ORFs were identified by tandem-SOM analysis and analyzed statistically using Genesifter software. ORFs in bold were confirmed by quantitative real-time PCR with independent biological replicates. All ORFs listed were upregulated.

ethers is to combine mechanistic and chemical information so that physiochemical properties of diphenyl ethers can be modified for greater bioavailability without compromising their specificity. Previous studies have reported on the ability of signature transcriptional profiles to categorize drug classes based on metabolic pressure (6). The identification of an increased number of genes allows for a greater number of features to be interrogated, thus providing a higher statistical

significance for signature profiling of a drug's mode of action. Thus, the next generation of compounds will be subjected to high-content multiple-feature profiling to prioritize screening efforts to those analogs with improved in vivo properties that maintain the desired metabolic effect on bacteria.

ACKNOWLEDGMENTS

This work was supported by NIH grants R01 AI-55298, R01 AI-044639, U01 AI-070383, NO1 AI-95385, and U54 AI-065357.

We acknowledge the postgenomic resources and services provided by the Rocky Mountain Regional Center of Excellence.

REFERENCES

1. **Banerjee, A., E. Dubnau, A. Quemard, V. Balasubramanian, K. S. Um, T. Wilson, D. Collins, G. D. Lisle, and W. R. Jacobs, Jr.** 1994. *inhA*, a gene encoding a target for isoniazid and ethionamide in *Mycobacterium tuberculosis*. Science **263:**227–230.
2. **Barry, C. E., III, R. E. Lee, K. Mdluli, A. E. Sampson, B. G. Schroeder, R. A. Slayden, and Y. Yuan.** 1998. Mycolic acids: structure, biosynthesis and physiological functions. Prog. Lipid Res. **37:**143–179.
3. **Barry, C. E., III, R. A. Slayden, A. E. Sampson, and R. E. Lee.** 2000. Use of genomics and combinatorial chemistry in the development of new antimycobacterial drugs. Biochem. Pharmacol. **59:**221–231.
4. **Basso, L. A., R. Zheng, J. M. Musser, W. R. Jacobs, Jr., and J. S. Blanchard.** 1998. Mechanisms of isoniazid resistance in *Mycobacterium tuberculosis*: enzymatic characterization of enoyl reductase mutants identified in isoniazid-resistant clinical isolates. J. Infect. Dis. **178:**769–775.
5. **Belisle, J. T., V. D. Vissa, T. Sievert, K. Takayama, P. J. Brennan, and G. S. Besra.** 1997. Role of the major antigen of *Mycobacterium tuberculosis* in cell wall biogenesis. Science **276:**1420–1422.
6. **Boshoff, H. I., T. G. Myers, B. R. Copp, M. R. McNeil, M. A. Wilson, and C. E. Barry III.** 2004. The transcriptional responses of *Mycobacterium tuberculosis* to inhibitors of metabolism: novel insights into drug mechanisms of action. J. Biol. Chem. **279:**40174–40184.
7. **Colangeli, R., D. Helb, S. Sridharan, J. Sun, M. Varma-Basil, M. H. Hazbon, R. Harbacheuski, N. J. Megjugorac, W. R. Jacobs, Jr., A. Holzenburg, J. C. Sacchettini, and D. Alland.** 2005. The *Mycobacterium tuberculosis iniA* gene is essential for activity of an efflux pump that confers drug tolerance to both isoniazid and ethambutol. Mol. Microbiol. **55:**1829–1840.
8. **Gruppo, V., C. M. Johnson, K. S. Marietta, H. Scherman, E. E. Zink, D. C. Crick, L. B. Adams, I. M. Orme, and A. J. Lenaerts.** 2006. Rapid microbiologic and pharmacologic evaluation of experimental compounds against *Mycobacterium tuberculosis*. Antimicrob. Agents Chemother. **50:**1245–1250.
9. **Heym, B., P. M. Alzari, N. Honore, and S. T. Cole.** 1995. Missense mutations in the catalase-peroxidase gene, katG, are associated with isoniazid resistance in *Mycobacterium tuberculosis*. Mol. Microbiol. **15:**235–245.
10. **Kremer, L., J. D. Douglas, A. R. Baulard, C. Morehouse, M. R. Guy, D. Alland, L. G. Dover, J. H. Lakey, W. R. Jacobs, Jr., P. J. Brennan, D. E. Minnikin, and G. S. Besra.** 2000. Thiolactomycin and related-analogues as novel anti-mycobacterial agents targeting KasA and KasB condensing enzymes in *Mycobacterium tuberculosis.* J. Biol. Chem. **275:**16857–16864.
11. **Li, X. Z., L. Zhang, and H. Nikaido.** 2004. Efflux pump-mediated intrinsic drug resistance in *Mycobacterium smegmatis*. Antimicrob. Agents Chemother. **48:**2415–2423.
12. **Mdluli, K., R. A. Slayden, Y. Zhu, S. Ramaswamy, X. Pan, D. Mead, D. D. Crane, J. M. Musser, and C. E. Barry III.** 1998. Inhibition of a *Mycobacterium tuberculosis* beta-ketoacyl ACP synthase by isoniazid. Science **280:**1607–1610.
13. **Quemard, A., J. C. Sacchettini, A. Dessen, C. Vilcheze, R. Bittman, J. William, R. Jacobs, and J. S. Blanchard.** 1995. Enzymatic characterization of the target for isoniazid in *Mycobacterium tuberculosis*. Biochemistry **34:**8235–8241.
14. **Rouse, D. A., Z. Li, G.-H. Bai, and S. L. Morris.** 1995. Characterization of the *katG* and *inhA* genes of isoniazid-resistant clinical isolates of *Mycobacterium tuberculosis*. Antimicrob. Agents Chemother. **39:**2472–2477.
15. **Slayden, R. A., and C. E. Barry III.** 2000. The genetics and biochemistry of isoniazid resistance in *Mycobacterium tuberculosis.* Microbes Infect. **2:**659–669.
16. **Slayden, R. A., and C. E. Barry III.** 2002. The role of KasA and KasB in the biosynthesis of meromycolic acids and isoniazid resistance in *Mycobacterium tuberculosis.* Tuberculosis (Edinburgh) **82:**149–160.
17. **Slayden, R. A., D. L. Knudson, and J. T. Belisle.** 2006. Identification of cell cycle regulators in *Mycobacterium tuberculosis* by inhibition of septum formation and global transcriptional analysis. Microbiology **152:**1789–1797.
18. **Slayden, R. A., R. E. Lee, J. W. Armour, A. M. Cooper, I. M. Orme, P. J. Brennan, and G. S. Besra.** 1996. Antimycobacterial action of thiolactomycin: an inhibitor of fatty acid and mycolic acid synthesis. Antimicrob. Agents Chemother. **40:**2813–2819.
19. **Slayden, R. A., R. E. Lee, and C. E. Barry III.** 2000. Isoniazid affects multiple components of the type II fatty acid synthase system of *Mycobacterium tuberculosis.* Mol. Microbiol. **38:**514–525.
20. **Sullivan, T. J., J. J. Truglio, M. E. Boyne, P. Novichenok, X. Zhang, C. F. Stratton, H.-J. Li, T. Kaur, A. Amin, F. Johnson, R. A. Slayden, C. Kisker, and P. J. Tonge.** 2006. High affinity InhA inhibitors with activity against drug-resistant strains of *Mycobacterium tuberculosis.* ACS Chem. Biol. **1:** 43–53.